Polymer Vol. 37 No. 4, pp. 565–572, 1996

0032-3861/96/$15.00 + 0.00

Fatigue and fracture behaviour of novel rubber modified epoxy resins

Adrian Lowe*, Oh-Hyok Kwon and Yiu-Wing Mai
Centre for Advanced Materials Technology, Department of Mechanical and Mechatronic Engineering, University of Sydney, NSW 2006, Australia
(Received 17 January 1995; revised 4 July 1995)

An extensive study has been performed assessing the structure and mechanical fracture and fatigue behaviour of rubber modified CIBA GEIGY GY260 cured with piperidine. The static fracture toughness was found to be unusually high, peaking at 2% rubber addition. The K_{Ic} value for the unmodified material was over three times higher than that of comparable epoxy systems, suggesting that a chemical modification may have taken place on the epoxy backbone. Structurally, the classical rubber particle morphology was not observed. Instead, a co-continuous structure was observed containing no discernible rubber concentrations. The structure of the low rubber content materials was significantly finer than that of the high rubber content materials, with the transition occurring at 2% rubber. A reaction mechanism has been proposed based on the hypothesis that the backbone modification has resulted in the formation of two types of reactive side groups that contribute to the overall toughness and solubility parameters of the material in different ways.

(Keywords: GY260; fracture toughness; structural models)

INTRODUCTION

Despite their inherent brittleness, epoxy resins have become one of the most important engineering materials of recent years. They are extensively used as matrix materials in composite materials and as adhesives in a multitude of applications. Their use has broadened due to an increased understanding of fracture and toughening processes and as a consequence, most epoxy resins are toughened in some form or another. Most epoxy resins are made from the reaction between bisphenol A and epichlorohydrin in an alkaline environment. Called diglycidyl ether of bisphenol A (DGEBA), these materials possess a wide range of mechanical properties and hence have a wide range of applications. For instance, a strength variation of over 100% can be attained by merely using different amine-based hardeners[1]. Epoxy resins are usually modified in one of three ways: the addition of hard particles[2–5]; the addition of elastomeric materials[5–8] or by the addition of thermoplastics[9–11].

The most common mechanism for toughening epoxies is by the addition of elastomers. This results in the rubber forming a dispersed particulate phase within the epoxy matrix. The size and distribution of these particles are controlled by energetic factors such as solubility parameters and surface energies, and also by processing factors such as cure time, cure temperature and cure pressure[12]. Chemical factors such as resin and hardener type also play a part. Perhaps the main toughening mechanism imparted by rubber addition is crazing around the particles caused by the presence of a strong tensile stress component at the particle which when stressed results in dilatational forces forming crazes along a plane normal to the loading axis. The energy required to form the crazes results in an increase in toughness whilst contributing to a general mechanical weakening of the material. McGarry *et al.*[8,13] found that small rubber particles ($< 0.1\ \mu m$) were not able to impart any toughening on epoxy resins, whereas larger ones could. They observed the biaxial yield behaviour of the toughened material and postulated that the biaxial yield locus could be represented by a pressure modified form of the Von Mises yield criterion i.e.

$$\tau_{oct} = \tau_o - \mu P \qquad (1)$$

where τ_{oct} is the octahedral shear stress, τ_o is the critical octahedral shear stress of the material, μ is the pressure coefficient (a measure of the sensitivity of the material to hydrostatic stress) and P is the mean applied stress. From this, small particle systems could be described by $\mu = 0.175$ and large particle systems by $\mu = 0.21$. Therefore, the degree of crazing (and consequently toughness) was found to be influenced by the size of the particles and could therefore be easily controlled. This mechanism has been used by many researchers[8,13–15] to explain toughening processes in various materials. Several other toughening mechanisms have also been identified including shear banding caused by crazing[15,16], rubber stretching and tearing[17] and cavitation[18].

Typically, DGEBA epoxies are modified using carboxyl-terminated butadiene acrylonitrile (CTBN) rubbers. This route was pioneered by McGarry and Sultan[8] who used CTBN of molecular weight 3000 and various DGEBA epoxies cured with piperidine, to

*Current address: Department of Engineering, Australian National University, Canberra 0200 ACT, Australia

achieve a ten-fold increase in toughness over a range of rubber contents. Liu and Nauman[19] used Epon 828 epoxy and diethylene triamine (DETA) hardener and found that the Izod impact strength actually decreased with increasing CTBN. Kinloch *et al.*[20] revealed a dynamic dependency in the DGEBA/CTBN/piperidine system by calculating the impact fracture toughness at different strike velocities and obtaining a near two-fold increase in toughness. Although toughness is enhanced, strength and modulus are reduced. Studies by Lee and Hodd[21] using CIBA-GEIGY MY720, CTBN1300×13 and piperidine revealed a clear decrease in strength and modulus with increasing rubber. The effect of particle size on the modulus of DGEBA/10% rubber/piperidine (various rubbers) was investigated by Pearson and Yee[22] who found that the modulus was independent of particle size. Previous studies[23] investigated the effect of matrix ductility (i.e., crosslinking density). Although no effect was found on the toughness of the bulk epoxy materials made from monomers of different molecular weights, a large dependence was observed on the addition of rubber.

The epoxy/CTBN/piperidine system is known to possess a relatively poor interfacial bond between the matrix and rubbery phases[24]. This is caused by the nature of the chemical reaction (chain extension reaction between the CTBN and epoxy until all carboxyl groups are consumed) producing limited crosslinking between the phases. Other rubber systems have been studied in work by Hwang *et al.*[25] who established that the higher the acrylonitrile content of the rubber, the smaller the resulting rubbery domain sizes. The possible influence of epoxy-based sub-zones existing within the rubbery domains was also reported. Recently, significant variations in toughness have been attained by chemical modification of the matrix and/or elastomer. For instance, Rezaifard *et al.*[26] reported that significant toughness enhancement could be achieved by using PMMA grafted natural rubber instead of CTBN.

Documentation relating to the fatigue behaviour of rubber modified epoxy resins is relatively scarce. Work by Manson *et al.*[27] showed that fatigue crack propagation rates were directly proportional to the crosslink density. Interestingly, further work[28] showed that for a CTBN modified DGEBA/amine system, there was no discernible fatigue toughening with increasing rubber content. This was tentatively attributed to energy dissipation mechanisms changing between high crack growth rates (monotonic) and low crack growth rates (fatigue). Hwang *et al.*[25] showed that for ETBN and ATBN toughened epoxies, an increase in fatigue toughness was attained with increasing rubber content and decreasing test frequency, probably due to the inability of the material to undergo beneficial hysteretic heating. Shear yielding of the epoxy matrix was revealed to be the dominant toughness mechanism in this instance.

TEST MATERIAL

The test material chosen for this study was CIBA GEIGY GY260—a commercially available DGEBA resin extensively used in the aerospace industry as an adhesive —cured with an amine hardener (piperidine) with a resin-to-hardener mixing ratio of 100 parts to 5 parts. To this was added varying amounts of HYCAR CTBN1300×13 elastomer of acrylonitrile content 27%, carboxyl content 2.4% and of solubility parameter 9.14 cal cm. Recent work[29] has shown this material system to be extremely unusual in that it possesses a substantially higher fracture toughness in the unmodified form than most standard epoxy resins[5,25], and tentative observations revealed that the addition of rubber will only enhance the fracture toughness up to around 2% whereupon further addition decreases the fracture toughness markedly. This is also extremely unusual as standard epoxy/rubber systems attain maximum toughness at around 15% rubber[26].

The epoxy was blended with a predetermined amount of rubber and degassed at 60°C before carefully mixing with the hardener and cast into large plates by using a preheated aluminium mould. The material was then cured at atmospheric pressure for 16 h at 120°C followed by a slow cure to room temperature. All plates that were found to be flaw free and devoid of trapped gas were then processed into the appropriate specimen dimensions.

EXPERIMENTAL AND RESULTS

Static fracture toughness

The static K_{Ic} behaviour was characterized at ambient temperature using compact tension test specimens containing a mid-plane crack, 25 mm long, as detailed in *Figure 1a*. The milled central groove was present in order to conserve dimensional similarity with the fatigue work detailed later. It also ensured a planar crack growth front. Additionally, a razor blade was used to propagate the crack a short distance prior to testing. This procedure ensured that crack growth would originate from a sharp crack tip. All tests were performed at a test rate of 1 mm min^{-1} within a servohydraulic test facility. Specimens of 0–30% rubber content were tested, and the expression for calculating K_{Ic} was as given by equation (2).

$$K_{Ic} = \frac{P_c}{B\sqrt{W}}\left[\frac{2+\frac{a}{W}}{\left(1-\frac{a}{W}\right)^{\frac{3}{2}}}\left(0.886+4.64\left(\frac{a}{W}\right)-13.32\left(\frac{a}{W}\right)^2+14.72\left(\frac{a}{W}\right)^3-5.6\left(\frac{a}{W}\right)^4\right)\right] \quad (2)$$

where P_c is the load required to fail the specimen and W, a and B are as defined in *Figure 1a*. Experimental scatter was small and the results obtained shown in *Figure 2*. Also shown are results obtained by Low and Mai[5] using GY250/CTBN/piperidine in the CT specimen configuration. All fracture toughness values are expressed in units of N mm $^{3/2}$ in order to provide easy comparison with previous and ongoing studies. However, they are also expressed in MPa$\sqrt{m}$ where appropriate, to aid comparison with other sources. The maximum fracture toughness of 140 N $mm^{-3/2}$ (4.42 MPa$\sqrt{m}$) clearly occurred at around 2% rubber inclusion, and at rubber contents greater than 15% the fracture toughness obtained is less than the bulk epoxy value of ~100 N mm $^{3/2}$ (3.16 MPa$\sqrt{m}$). This bulk value is substantially higher than that for GY250, suggesting that the differences in the material are not subtle. The anomalous results shown in *Figure 2* were unexpected and so were repeated several times using several different material batches on two

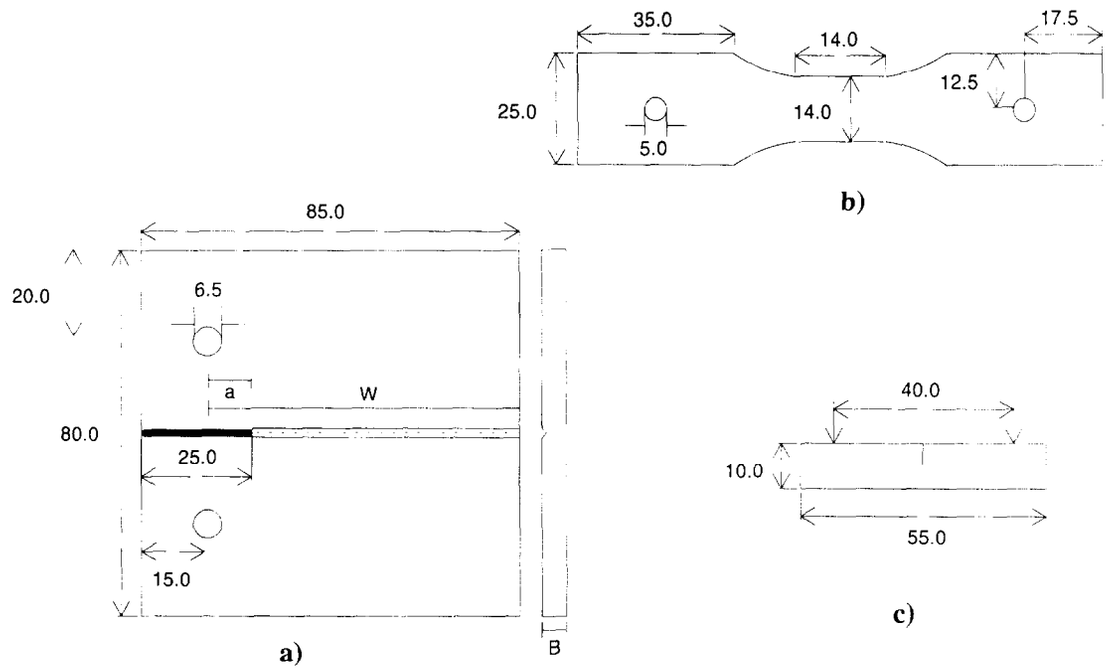

Figure 1 Detailing the test geometries used (all dimensions in mm). (a) Compact tension specimen where a (crack length) = 10 mm, W (effect length) = 70 mm and B (thickness) = 6 mm. (b) Tensile dogbone test specimen (thickness = 6 mm). (c) Dynamic fracture toughness specin (thickness = 6 mm)

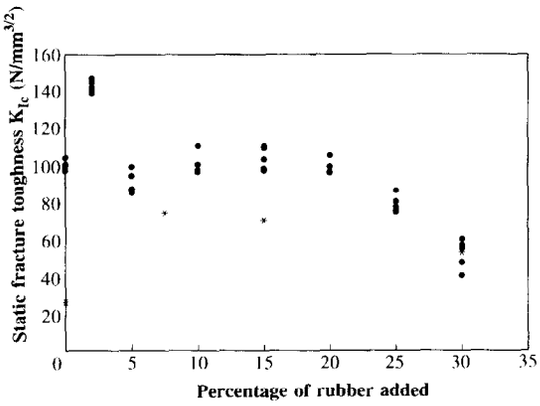

Figure 2 Variation of static fracture toughness with rubber content for GY260 (●) and GY250 (*)[5] cured with piperidine

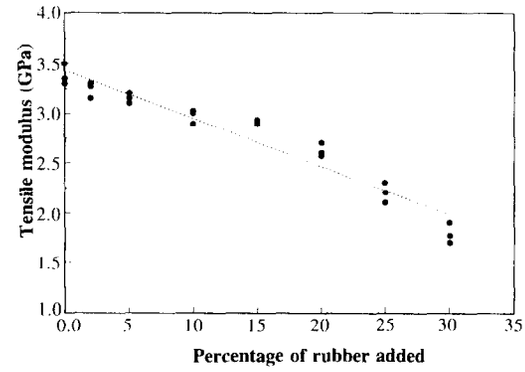

Figure 3 Variation of tensile Young's modulus with rubber content for GY260/piperidine

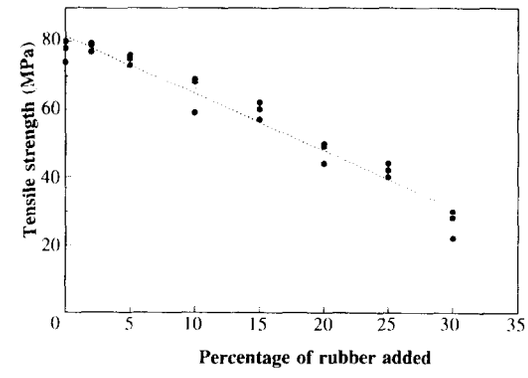

Figure 4 Variation of tensile strength with rubber content for GY260/piperidine

different test machines. No variation from the original data was found. These results correlate well with ref. 29 and with subsequent, unpublished tests and can therefore be classed as reliable.

Static tensile behaviour

The tensile test specimen shown in *Figure 1b* is a variation on the dogbone test geometry comprising two end regions waisted down to a central parallel region. The specimen was originally designed for low cycle fatigue testing, with the central region designed for application of a clip gauge. However, tests on other materials[30] revealed this geometry to also yield excellent monotonic data. The static modulus, strength and stress/strain behaviour were determined for various rubber contents at ambient temperature, at a rest rate of 1 mm min^{-1} using a servohydraulic test facility.

Figures 3 and *4* show that both modulus and strength decrease with increasing rubber content in a linear manner; these values and trends being similar to other rubber modified systems[31,32]. This linearity indicates that modulus and strength are not affected by rubber addition in the same way as the toughness behaviour. *Figure 5* presents typical stress/strain curves seen at each rubber content. Wholesale drawing and necking of materials

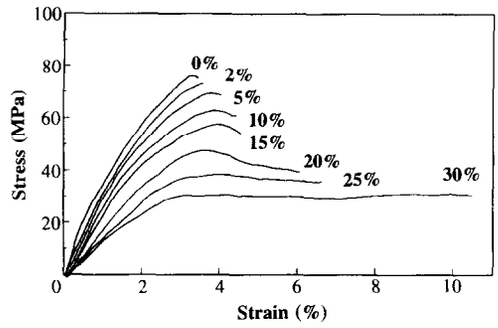

Figure 5 Stress/strain behaviour of GY260/piperidine of various rubber contents

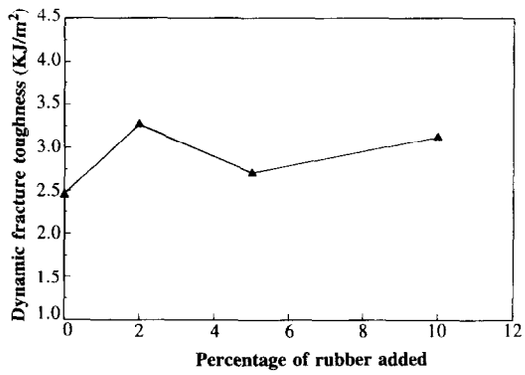

Figure 6 Variation of dynamic fracture toughness with rubber content for GY260/piperidine

containing rubber contents greater than 2% starts to occur, suggesting that different deformation mechanisms may be at work.

Dynamic fracture toughness

Understanding the dynamic fracture properties of an adhesive material such as GY260 is paramount to good design as it characterizes mechanical behaviour as a result of impact or collision with other entities. Standard Charpy test specimens (*Figure 1c*) were used to obtain dynamic fracture toughness values with the central crack machined using a fine milling tool followed by use of a razor blade to propagate a sharp crack front. As Charpy and related fracture values cannot be regarded as material parameters due to the effect of specimen size, Williams *et al.*[33–35] derived an expression that related the impact energy absorbed by the specimen, U, to the true fracture toughness, G_{Ic}, as shown in equation (3).

$$U = U_k + G_{Ic}BW\phi \tag{3}$$

where B is the specimen thickness, W is the specimen width and U_k represents the kinetic energy lost on impact. ϕ is a geometric factor dependent on the compliance of the specimen and the length of the central crack, a:

$$\phi = \frac{C}{dC/d(a/W)} \tag{4}$$

hence a plot of U vs ϕ will yield G_{Ic}.

Materials of rubber content 0%, 2%, 5% and 10% were treated at ambient temperature. A Zwick Charpy impact testing facility located within a thermally controlled environment was used, of full scale 0.5 J and a test velocity of 2.93 m s^{-1}. *Figure 6* presents the variation of dynamic fracture toughness with rubber content and shows that maximum fracture toughness is achieved using 2% rubber content. Other unpublished work[36] has shown that this is also the case with material tested at temperatures ranging from −80°C to 30°C.

Fatigue behaviour

Characterization of fatigue crack growth behaviour as a function of rubber content was achieved using high cycle fatigue of compact tension test specimens identical to those used for the static fracture toughness work. All tests were performed at ambient temperature, at a test frequency of 1 Hz and at a load ratio (R) of 0.1, where R = minimum load/maximum load. Unlike previous work[37], an electrically conducting grid mechanism could not be used for crack growth monitoring as the crack tip plastic deformation observed at high rubber contents was greater than the deformation capabilities of the conducting medium. Conversely, at low rubber content (2%), deformation was so small that the crack would often propagate past the grid bar before a break was recorded. Crack growth was therefore monitored manually, i.e., by illuminating the *in situ* specimen from behind and identifying the crack front with a very fine marking instrument after a predetermined number of cycles. The milled central groove ensured a regular crack growth front. Data were not forthcoming from the 0% rubber material, as crack growth could not be adequately controlled. Crack growth was easily characterized using the Paris Power Law[38]:

$$\frac{da}{dN} = C\Delta K^n \tag{5}$$

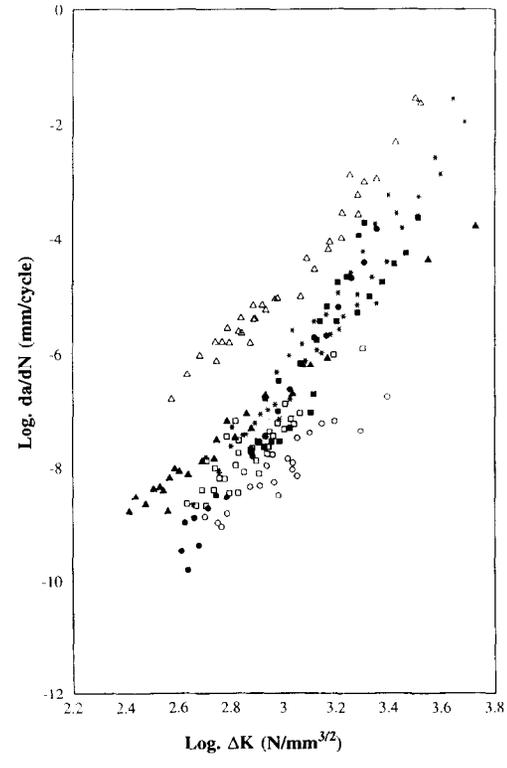

Figure 7 Variation of fatigue crack growth rate with applied ΔK for GY260/piperidine of various rubber contents: ○ = 2%, □ = 5%, ● = 10%, ■ = 15%, * = 20%, ▲ = 25% and △ = 30% rubber

Table 1 Detailing the fatigue constants C and n and the maximum applied ΔK obtained from the fatigue experiments

Rubber content (%)	C	n	ΔK_{max} ($N\,mm^{-3/2}$)	($MPa\sqrt{m}$)
2	−18.05	2.89	29.67	0.938
5	−19.22	4.00	27.11	0.857
10	−28.84	7.37	28.50	0.901
15	−26.19	6.45	33.45	1.058
20	−25.15	6.21	39.65	1.254
25	−18.34	3.91	41.68	1.318
30	−20.32	5.19	33.78	1.068

where da/dN is the amount of crack growth observed per cycle, ΔK is the applied stress intensity range, C is a proportionality factor and n is the fatigue coefficient, defining the fatigue crack growth characteristics of the material. ΔK is varied by varying the applied peak load while keeping R constant. Clearly, as ΔP is kept constant throughout the test, then ΔK will increase with crack length up to a value ΔK_{max} at which catastrophic failure occurs. The fatigue data obtained is shown in *Figure 7*, with the values of n, C and ΔK_{max} for each rubber content shown in *Table 1*.

FRACTOGRAPHIC EXAMINATION

Fractographic examination was performed using small areas cut from static fracture toughness test specimen fracture surfaces. The images were enhanced by staining the specimens with osmium tetroxide for 24 h prior to examination. This procedure stains any rubber based compounds present, resulting in greater image contrast. *Figure 8a* shows a fracture surface taken at 100 000× magnification of GY260 + 0% rubber and shows that the structure of the material consists of small microdomain-type structures as if a degree of phase separation has occurred. The equivalent back scattered image is shown in *Figure 8b* and is basically featureless. Fracture surfaces of GY260 containing 2%, 15% and 30% rubber are shown in *Figures 8c*, *e* and *g*, respectively, together with equivalent back scattered images of the same areas in *Figures 8d*, *8f* and *8h*.

The classical rubber toughened structure of well-defined rubber spheres within a homogeneous epoxy matrix evidently does not form in this system, and the 2% material appears structurally identical to the 0% material. The light band bisecting *Figure 8c* is merely a crack front. The 15% and 30% images show a greater degree of surface topography than the 0% and 2% materials, suggesting an increased amount of deformation to fracture. However, there is no evidence of rubber rich regions. The purpose of obtaining back scattered images is to greatly enhance contrast differences between elements of different atomic number. The greater the difference, the greater the contrast, e.g., carbon and osmium. As there are no great contrast differences in *Figures 8d*, *8f* and *8h*, the osmium appears to have uniformly dispersed. In these systems, the only linkage that can be possibly stained by osmium tetroxide is the rubber linkage, and so there must be a uniform distribution of rubber within the materials. Furthermore, *Figure 8b* was obtained at the same contrast level as the other back scattered images and therefore shows a uniform osmium distribution. The only explanation for this is that there must be a rubber based linkage within the epoxy molecule, i.e., some form of grafting has taken place, as osmium tetroxide is not known to stain piperidine linkages. Further fractographic analysis has subsequently shown there to be no difference between fracture surfaces and fatigue surfaces.

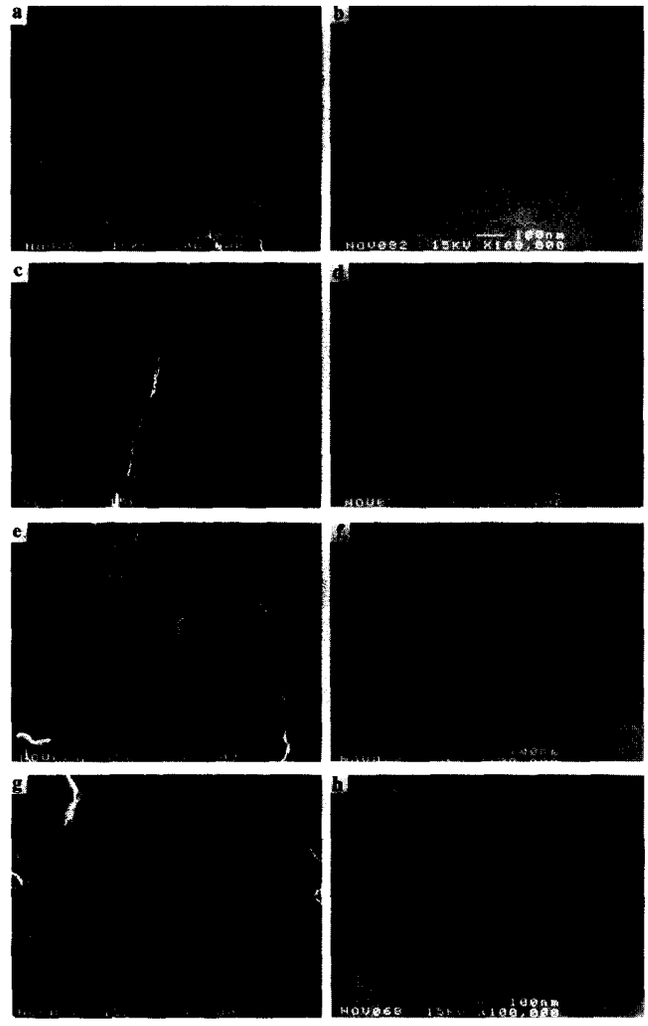

Figure 8 Scanning electron microscope images of GY260/piperidine fracture surfaces of various rubber contents under normal (SEI) and back scattered (BS) views. (a) 0% rubber (SEI), (b) 0% rubber (BS), (c) 2% rubber (SEI), (d) 2% rubber (BS), (e) 15% rubber (SEI), (f) 15% rubber (BS), (g) 30% rubber (SEI), and (h) 30% rubber (BS)

DISCUSSION

Fracture data

The strength and modulus data in *Figures 3* and *4* show a linear decrease with increasing rubber content, typical of most epoxy/rubber systems[21]. Their magnitudes are also comparable. It would appear that the structural anomalies which clearly affect toughness, hold no influence over strength or modulus, suggesting that the fracture mechanics have remained unaffected. However, the stress/strain curves have revealed that necking and drawing occur only after the addition of rubber contents greater than 2%, which corresponds to the change in structural morphology observed in *Figure 8*.

If the impact fracture toughness data used for *Figure 5* is translated into dynamic K_{Ic} data by means of the elastic relation $K_{Ic} = \sqrt{(EG_{Ic})}$, then the static and dynamic toughness values are seen to be similar for the higher rubber content materials, whereas for the 0% and 2% materials, the dynamic toughness values are substantially lower than the static values. This would imply that the strain rate dependence of the two sets of materials is different.

Fatigue data

From *Figure 7*, it is evident that fatigue behaviour is influenced by the amount of rubber present. There is no fatigue modelling work readily available that defines fatigue parameters in terms of rubber content; however, the influence of rubber content can easily be accounted for by using the corresponding variations in E and K_{Ic}. A simple curve fitting exercise can be performed on the fatigue data using equation (5) by modifying the values of C and n to account for rubber content (%) in terms of tensile modulus, E. From *Figure 3*, the relationship between E and % is linear, as described by equation (6):

$$E = -0.049\% + 3.431 \tag{6}$$

and so

$$\frac{da}{dN} = \check{C}\Delta K^{\check{n}} \tag{7}$$

where $\check{C} = 26.56E^3 - 185.39E^2 + 411.42E - 311.099$ and $\check{n} = -11.95E^3 + 88.50E^2 - 213.40E + 173.13$.

These expressions were derived by fitting third-order polynomials to the values presented in *Table 1*.

In theory, if there was perfect agreement between the experimental data and equation (7), a normalized plot of $1/\check{n}.\ln((da/dN)/\check{C})$ vs $\ln \Delta K$ should yield a straight line of gradient 1 passing through the origin. *Figure 9* presents the normalized data on the same scale as *Figure 7*, revealing a limited degree of homogenization in the data. Wnuk[39] derived an expression especially for polymeric materials based on the Paris law that accounted for both K_{Ic} and viscoelastic responses, i.e.

$$\frac{da}{dN} = C_1\left(\frac{\Delta K}{K_{Ic}}\right)^m + C_2\left(\frac{\Delta K}{K_{Ic}}\right)^n (f^{-1}) \tag{8}$$

where f is the test frequency and the two material constants, C_1 and C_2, represent the in-phase (elastic) and out-of-phase (inelastic) components of fatigue compliance, respectively. For purely elastic materials, the second term is negligible and the expression reduces to a basic Paris law. As the anomalous K_{Ic} behaviour may influence the fatigue behaviour, account of this must be taken. *Figure 10* shows the experimental data expressed as a plot of $\ln da/dN$ vs $\ln \Delta K/K_{Ic}$ (dimensionless) with *Table 2* giving the values obtained for C, n and $(\Delta K/K_{Ic})_{max}$. Interestingly, there is a perfectly linear correlation between C and n, i.e.

$$C = 1.90n - 8.97 \tag{9}$$

and so repeating the previous curve fitting exercise, and using equation (9):

$$\frac{da}{dN} = \left(\frac{\Delta K}{K_{Ic}}\right)^{\alpha}(1.9\alpha - 8.97) \tag{10}$$

where $\alpha \equiv \check{n}$ and is now the only parameter required to describe the observed fatigue behaviour. A normalized plot of $1/\alpha.\ln((da/dN)/(1.9\alpha - 8.97))$ vs $\ln(\Delta K/K_{Ic})$ can be obtained, as shown in *Figure 11*. Here, the 2% material clearly behaves differently to all other compositions and this appears to be a direct consequence of the abnormally high fracture toughness value seen in *Figure 2*. This phenomenon is an unusual one and may be due to structural anomalies present in the 2% material.

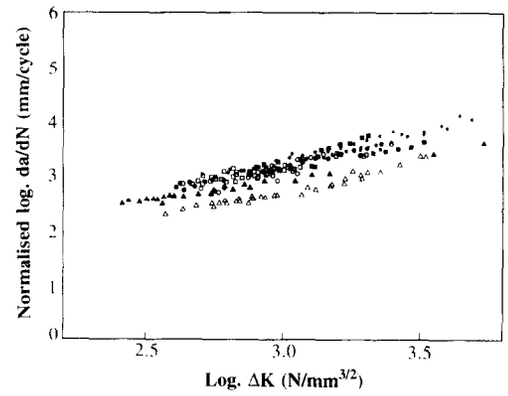

Figure 9 Previous fatigue data presented in normalized form using curve fitting procedures to obtain $\check{C}$ and $\check{n}$: ○ = 2%, □ = 5%, ● = 10%, ■ = 15%, * = 20%, ▲ = 25% and △ = 30% rubber

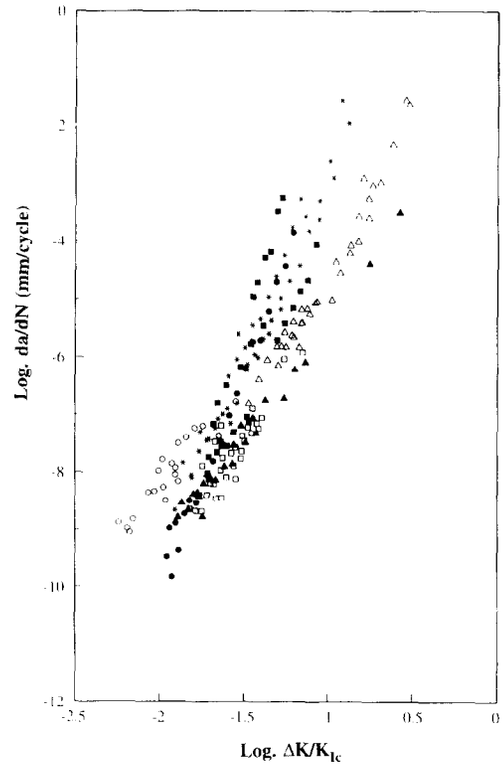

Figure 10 Variation of fatigue crack growth rate with applied $\Delta K/K_{Ic}$ for GY260/piperidine of various rubber contents: ○ = 2%, □ = 5%, ● = 10%, ■ = 15%, * = 20%, ▲ = 25% and △ = 30% rubber

Structural observations

From the fractographic analysis, it appears that there are some structural differences between low rubber content and high rubber content materials. The structure of the 0% and 2% materials appears finer than that of the more rubbery materials, and this phenomenon clearly affects the toughness of the material but not the

Table 2 Detailing the fatigue constants C and n and the maximum applied ΔK obtained from the fatigue experiments after accounting for K_{Ic}

Rubber content (%)	C	n	$(\Delta K/K_{Ic})_{max}$
2	−1.51	3.35	0.2119
5	−1.39	4.00	0.3152
10	4.80	7.37	0.2969
15	3.26	6.34	0.3413
20	3.37	6.31	0.4130
25	−1.51	3.90	0.5632
30	0.66	5.19	0.5926

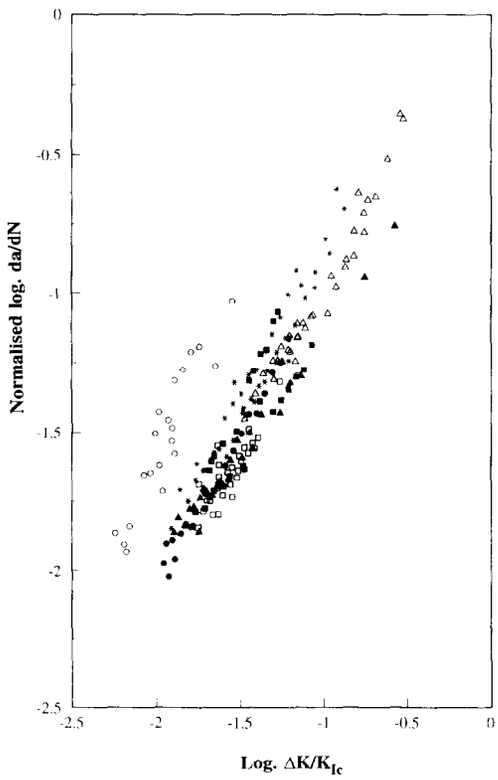

Figure 11 Fatigue data presented in normalized form after accounting for K_{Ic} and after using curve fitting procedures to obtain α: ○ = 2%, □ = 5%, ● = 10%, ■ = 15%, * = 20%, ▲ = 25% and △ = 30% rubber

strength or modulus. The fact that large rubber particles are absent is not unexpected as the high acrylonitrile content of the test rubber is known to significantly reduce the rubber domain sizes[25]. However, there is a total absence of rubber particles of any size. It is possible that there has been some form of chemical modification imparted onto the epoxy backbone and/or side groups to improve the interfacial bond between the matrix and rubber, which is known to be poor in this type of material[24]. This would explain the enhanced toughness observed, and may have also altered the solubility parameter of the epoxy to such a degree that formation of distinct rubber domains has been suppressed in favour of the co-continuous/microdomain structure seen in *Figure 8*. If this modification results in enhanced crosslinking on curing, then this explains the high toughness observed in the 0% rubber material.

It is also feasible that this proposed modification has resulted in two types of reactive groups on the epoxy, i.e., a type A group, present in the original unmodified resin,

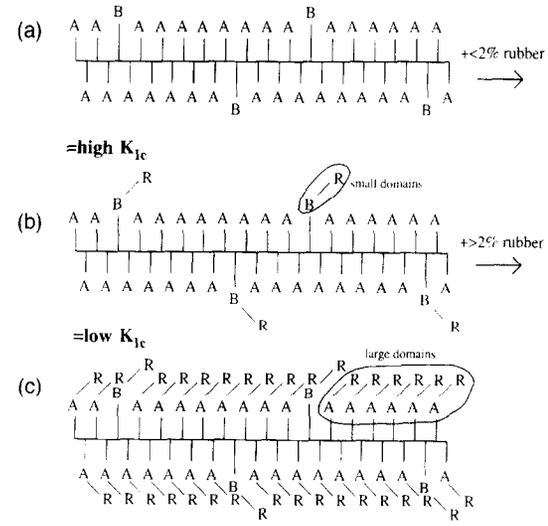

Figure 12 Schematically illustrating the proposed reaction mechanism in GY260/piperidine on the addition of rubber. (a) Base epoxy molecule containing standard side groups (A) and a small number of different side groups (B) created by modification of the molecule. (b) Addition of up to 2% rubber results in reaction of the B groups to form small microdomains of relatively high toughness within the crosslinked epoxy structure. (c) Causes reaction of some to all of the A groups, resulting in the formation of larger microdomains of lower toughness

that would normally form the classical particulate structure on curing, and a type B group created by the modification, that when reacted will form a significantly different bond with the rubber. If the amount of B groups is small, then it is possible that 2% rubber addition represents the threshold at which saturation occurs (i.e., all the B groups have reacted). Further rubber additions may result in reaction of the A groups, theoretically inducing the material to form rubber particles. However, as the presence of the modification has most likely changed the solubility parameter of the epoxy, the formation of particles would be suppressed and instead, a co-continuous structure of relatively low toughness has formed. This structure may also be easily deformable, thus explaining the necking and drawing observed in high rubber content materials during the tensile test program. This proposed reaction mechanism is schematically detailed in *Figure 12*. The high toughness seen in the 0% material would then probably be caused by preferential reaction of the B groups to form a highly crosslinked structure.

CONCLUSIONS

The results presented in this study have clearly shown that GY260/piperidine with and without rubber modification is a very unusual material. The expected rubber particle distribution has not occurred, and instead there appears to be a co-continuous phase development throughout which the added rubber has homogeneously distributed. Its structure, toughness and fatigue behaviour are anomalous and show that low rubber content materials behave differently to high rubber content materials, with the transition occurring at around 2% rubber addition. These anomalies are not observed in the modulus or strength behaviour. The evidence points to there being some form of modification occurring on the epoxy molecule that has altered the phase separation characteristics on curing, resulting in a microdomain/

co-continuous phase distribution rather than the classical rubber particle structure.

Compared to other epoxies, the toughness of GY260/piperidine is very high, and so the bonding between epoxy molecules and the hardener has been substantially improved. A tentative chemical reaction model has been developed to explain all these phenomena, and assumes the existence of more than one type of reactive side group on the epoxy backbone. Fatigue analysis of this system has resulted in a modified Paris law being developed containing a single defining parameter that accounts for changes in the modulus of the material, and hence, changes in rubber content. The fatigue response of GY260/piperidine + 2% rubber was found to be different to all other compositions.

ACKNOWLEDGEMENTS

The authors wish to express their sincere gratitude to the Aeronautical Research Laboratories, Melbourne and, in particular, Dr Francis Rose for financial support and technical guidance throughout the duration of this work.

REFERENCES

1 Lee, W. H. and Neville, K. 'Handbook of Epoxy Resins', McGraw-Hill, New York, 1967
2 Spanoudakis, J. and Young, R. J. *J. Mater. Sci.* 1984, **19**, 473
3 Mallick, P. K. and Broutman, L. J. *Mater. Sci. Eng.* 1975, **18**, 63
4 Young, R. J. and Beaumont, P. W. R. *J. Mater. Sci.* 1975, **10**, 1343
5 Low, I. M. and Mai, Y.-W. *Comp. Sci. Tech.* 1988, **33**, 191
6 Mostovoy, S., Ripling, E. J. and Bersch, C. F. *J. Adhesion* 1971, **4**, 125
7 Ripling, E. J., Mostovoy, S. and Corten, H. T. *J. Adhesion* 1971, **3**, 107
8 Sultan, J. N. and McGarry, F. J. *J. Polym. Eng. Sci.* 1973, **13**, 29
9 Bucknall, C. B. and Partridge, I. K. *Polymer* 1983, **24**, 639
10 Bucknall, C. B. and Partridge, I. K. *Br. Polym. J.* 1983, **15**, 71
11 Yamanaka, K. and Inoue, T. *Polymer* 1989, **30**, 662
12 Yee, A. F. and Pearson, R. A. *J. Mater. Sci.* 1986, **21**, 2462
13 Sultan, J. N., Liable, R. C. and McGarry, F. J. *Polym. Symp.* 1971, **16**, 127
14 Riew, C. K., Siebert, A. R. and Smith, R. W. *Am. Chem. Soc. Adv. Chem. Ser.* 1976, **154**, 326
15 Bucknall, C. B. and Yoshii, T. *Br. Polym. J.* 1978, **10**, 122
16 Bucknall, C. B. 'Toughened Plastics', Applied Science, London, 1977
17 Kunz-Douglass, S., Beaumont, P. W. R. and Ashby, M. F. *J. Mater. Sci.* 1980, **15**, 1109
18 Kinloch, A. J., Shaw, S. J. and Tod, D. A. *Polymer* 1983, **24**, 1342
19 Liu, S. H. and Nauman, E. B. *J. Mater. Sci.* 1991, **26**, 6581
20 Kinloch, A. J., Kodokian, G. A. and Jamarani, M. B. *J. Mater. Sci.* 1987, **22**, 4111
21 Lee, W. H. and Hodd, K. A. *J. Mater. Sci.* 1992, **27**, 4582
22 Pearson, R. A. and Yee, A. F. *J. Mater. Sci.* 1991, **26**, 3828
23 Pearson, R. A. and Yee, A. F. *J. Mater. Sci.* 1989, **24**, 2571
24 Chan, L. C., Gillham, J. K., Kinloch, A. J. and Shaw, S. J. *Am. Chem. Soc. Adv. Chem. Ser.* 1984, **208**, 235
25 Hwang, J. F., Manson, J. A., Hertzberg, R. W., Miller, G. A. and Sperling, L. H. *Polym. Eng. Sci.* 1989, **29**, 1466
26 Rezaifard, A. H., Hodd, K. A., Tod, D. A. and Barton, J. M. *Int. J. Adhesion Adhesives* 1994, **14**, 153
27 Kim, S. L., Skibo, M. D., Manson, J. A., Hertzberg, R. W. and Janiszewski, J. *Polym. Eng. Sci.* 1978, **18**, 1093
28 Shah, D. N., Atalla, G., Manson, J. A., Connelly, G. M. and Hertzberg, R. W. *Am. Chem. Soc. Adv. Chem. Ser.* 1984, **208**, 117
29 Daghyani, H. R., Ye, L., Mai, Y. W. and Wu, J. S. *J. Mater. Sci. Lett.* 1994, **13**(18), 1330
30 Lowe, A. unpublished work
31 Selby, K. and Miller, L. E. *J. Mater. Sci.* 1975, **10**, 12
32 Chen, T. K. and Jan, Y. H. *J. Mater. Sci.* 1991, **26**, 5848
33 Kinloch, A. J. and Williams, J. G. *J. Mater. Sci.* 1980, **15**, 987
34 Plati, E. and Williams, J. G. *Polym. Eng. Sci.* 1975, **15**, 470
35 Marshall, G. P., Williams, J. G. and Turner, C. E. *J. Mater. Sci.* 1973, **8**, 949
36 Kwon, O. K. Undergraduate Thesis, Department of Mechanical and Mechatronic Engineering, University of Sydney, 1993
37 Lowe, A. and Mai, Y.-W. in 'Proceedings of the Ninth International Conference on Composite Materials (ICCM/9)', Madrid, July 1993 (Ed. A. Miravete), University of Zaragoza, Woodhead Publishing Ltd, 1993
38 Paris, P. C. and Erdogan, F. *J. Bas. Eng. Trans. ASME Ser. D* 1963, **85**, 528
39 Wnuk, M. P. *J. Appl. Mech.* 1974, **41**, 234